DOI 10.1007/s10812-019-00912-3
Journal of Applied Spectroscopy, Vol. 86, No. 5, November, 2019 (Russian Original Vol. 86, No. 5, September–October, 2019)

OPTICAL DESIGN OF IMAGE POLYCHROMATOR FOR SPATIALLY RESOLVED IMAGING SPECTROSCOPY

I. M. Gulis* **and A. G. Kupreyeu** UDC 681.785.554

We have developed a basic approach and a design for snapshot recording of multispectral information, based on a dispersive polychromator with mirror objectives. By means of numerical modeling, we have shown that the halfwidth of the blur spots for 11 spectral bands in the 400–700 nm range, for imaging points at the center and on the periphery of the object field, is not greater than 15 μm for a focal length of the camera mirror equal to 100 mm. Owing to the use of simple optical elements, the design can serve as the basis for making inexpensive devices for a wide range of spatially resolved imaging spectroscopy applications.

Keywords: *multispectral imaging, dispersive image polychromator.*

Introduction. In spatially resolved imaging spectroscopy, a popular method for generating a data cube (the dependences of the intensity $I(x, y, \lambda)$ on the coordinates of the object image x, y and the radiation wavelength λ) is to record a set of spectra $I(x_i, y_i, \lambda)$ for a set of image points (x_i, y_i) [1, 2]. Another method presumes that for a set of relatively narrow spectral bands with centers at λ_k, a set of "quasimonochromatic images" $I(x, y, \lambda_k)$ is recorded: "multispectral imaging" [3]. For many problems of practical importance, obtaining a set of multispectral images is a more convenient way to analyze spectral and spatial information about an object. In the simplest variant, multispectral imaging is reduced to recording a set of images through optical filters [4]. However, such an approach has a number of fundamental limitations, due to incomplete suppression of light transmission beyond the spectral band nominally to be selected by an individual optical filter. The indicated deficiency becomes an even greater obstacle to obtaining reliable spectral and spatial information as the widths of the bands to be selected by the optical filter decrease (as the spectral resolution increases): the background transmission integrated over the spectrum may be comparable with the spectral transmission within the narrow band to be selected (or may even exceed it). Accordingly, there is certainly interest in a design based on diffraction spectral filtering which can provide higher spectral resolution and effective suppression of the background. Such dispersive devices can be called image monochromators. Multispectral imaging is reduced in this case to sequential recording of images for a set of λ_k, selected when tuning the monochromator. Fundamentally new opportunities are opened up by an approach which is actively under development today, aimed at recording the entire data cube $I(x, y, \lambda)$ in one measurement (snapshot hyperspectroscopy) [5]. Besides the obvious gain in capability for making on-the-fly measurements (a short time is required to obtain the data cube), such an approach lets us also record $I(x, y, \lambda)$ for a broad class of nonstationary objects.

A dispersive device letting us take snapshots of a set of quasimonochromatic images is appropriately called an image polychromator. Some conceptual proposals for the circuit architecture and a prototype have been developed, for example in [6]. At the same time, obviously in order to realize a feasible device, we need to solve the problem of generating a set of images for the selected spectral bands with minimal aberration distortion and optimal focusing for all the field points on the photodetector.

In this paper, we propose an optical layout for an image polychromator and analyze the quality of the image formed by the device.

Design of the Optical System. We used mirror optics in the optical layout (Fig. 1), which eliminates chromatic aberration and also lets us record in spectral ranges from the UV to the IR. The layout is intended for operation using collimated beams (with the object at infinity), but by using additional entrance optics can be adapted for operation with objects located at arbitrary distances from the entrance aperture.

*To whom correspondence should be addressed.

Belarusian State University, 4 Nezavisimost′ Ave., Minsk, 220030, Belarus; email: gulis@bsu.by. Translated from Zhurnal Prikladnoi Spektroskopii, Vol. 86, No. 5, pp. 813–816, September–October, 2019. Original article submitted May 30, 2019.

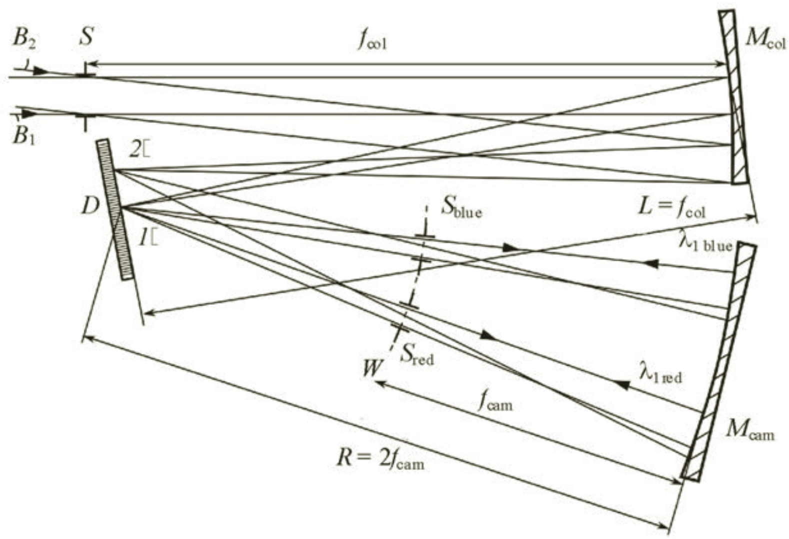

Fig. 1. Diagram showing the layout of the image polychromator: S is the entrance aperture; B_1 and B_2 are beams from the center and the edge of the field; M_{col} is the collimator mirror with focal length f_{col}; D is the diffraction grating; M_{cam} is the camera mirror with focal length f_{cam}; S_{blue} and S_{red} are slits for spatial filtering of chromatic beams with arbitrary wavelengths λ_{blue} and λ_{red}; 1' and 2' are the points near the surface of diffraction grating D at which beams B_1 and B_2 are focused; W is the focal surface of the mirror M_{cam}; the plane of dispersion is parallel to the plane of the figure.

One feature of the layout is that the diffraction grating D is positioned at distance L from the collimator objective M_{col}, equal to the focal length f_{col} of this objective, and so the objective M_{col} forms an image of the object at infinity near the surface of diffraction grating D. Then the layout of the spectrograph is built as spherocentric: the center of the spherical mirror (the camera objective M_{cam}) coincides with the center of grating D [7].

The system of elements, including the entrance slit S, the collimator mirror M_{col}, the diffraction grating D located at a distance f_{col} from it, the camera mirror M_{cam}, and the slit (for example, S_{blue}) at a distance f_{cam} from the camera mirror, fulfill the function of a monochromator tuned to the wavelength λ_k for all beams incident on S. The images of objects at infinity on the diffraction grating are denoted as 1' и 2'. The spherical camera mirror M_{cam}, located at the distance $R = 2f_{cam}$ from the diffraction grating, re-images this pattern into the region of the diffraction grating with spectral filtering determined by the slit S, on the focal plane W of the objective M_{cam}. Thus the system can be considered as an image monochromator. Placing several slits on W (S_{blue}, ... , S_{red}) let us obtain an image in a set of spectral bands corresponding to different λ_k. Separation of the beams going in the direction of M_{cam} and reflected from it and going to the detector is accomplished by tilting the mirror M_{cam} at a small angle in the plane perpendicular to the plane of dispersion. In order for aberrations introduced by such a tilt to be minimal, the tilt angle for M_{cam} also should be minimal. Note that M_{cam} fulfills the function of the camera objective, providing spectral selection, and it forms narrow-band images.

For realization of an image polychromator (a device letting us record a set of images corresponding to different λ_k), we need to spatially separate these images. To do this, instead of slits S_{blue}, ... , S_{red} we use a set of mirrors, where the tilt of each mirror specifies a direction toward an individual array in the photodetector (combining them on the same detector does not seem possible due to the tilt of the normal to the diffraction grating relative to the optic axes of the diffracted beams).

Based on the indicated approach, we developed an optical layout for a multispectral polychromator (Fig. 2). Entrance aperture 1 is a circular opening of diameter 3 mm. The radius of the collimator mirror is 400 mm, the radius of the camera mirror is 200 mm (focal length 200 mm and 100 mm). The diffraction grating (1200 lines/mm) operates in –1st order and is perpendicular to the optic axis in the section before the grating. The tilt angle of the camera mirror is $\alpha/2 = 1.6^{o}$. The tilt of mirrors 6 was selected so that they deflected the imaging beams in the x direction (downward) at angles close to the normal to the plane of dispersion; 11 mirrors 6 have a square shape and size 3 × 3 mm, resulting in generation of 11 spectral bands

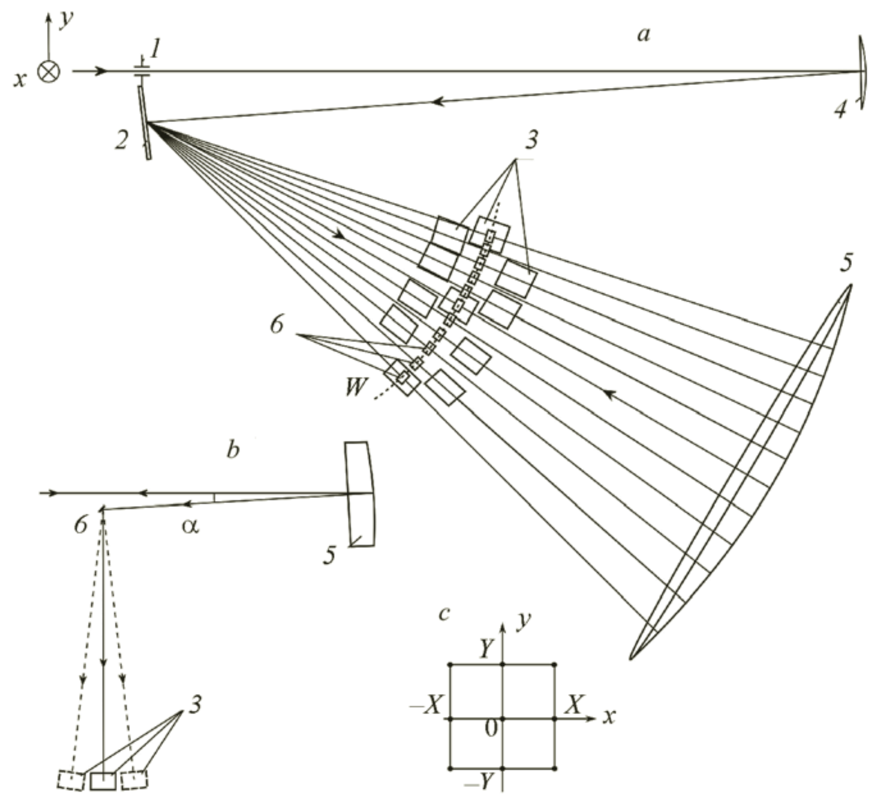

Fig. 2. Optical layout of image polychromator: a) top view, b) diagram showing travel of axial ray of the beam with λ = 550 nm (dashed line represents travel of axial rays of beams 520 nm and 580 nm, and also the corresponding detectors), c) points of the object field for which we analyzed the blur spots (the coordinate system corresponds to Fig. 2a); 1) entrance aperture, 2) diffraction grating, 3) detectors for recording individual spectral bands (partially shown in Fig. 2b), 4) collimator mirror, 5) camera mirror, 6) the mirrors are functional analogs of the slits (one is shown in Fig. 2b); α is the exit angle from the plane of dispersion; the arrows show propagation of the axial rays of chromatic beams; *W* is the focal surface of objective 5.

TABLE 1. Halfwidth of Blur Spots for Object Field Points (Fig. 2c) in *x* and *y* Coordinates (*x*/*y*), μm

λ, nm	(0, 0)	(0, *Y*)	(0, –*Y*)	(*X*, 0)	(–*X*, 0)	(*X*, *Y*)	(*X*, –*Y*)	(–*X*, *Y*)	(–*X*, –*Y*)
400	3/3	4/8	4/4	13/5	4/2	15/12	12/7	6/5	5/3
430	2/2	4/6	5/5	7/4	2/6	8/8	11/5	3/9	4/8
460	3/4	7/4	9/10	7/2	2/6	7/8	14/8	7/4	5/13
490	3/5	5/8	6/7	8/2	2/8	9/8	11/5	3/12	5/10
520	2/2	8/4	6/7	6/4	2/4	7/10	11/6	9/3	4/10
550	1/3	5/8	4/5	6/4	2/8	8/8	11/5	4/13	3/9
580	2/4	6/6	7/9	7/4	2/11	7/8	11/5	6/11	6/15
610	2/2	8/4	4/5	9/3	5/2	8/8	13/7	12/1	3/4
640	2/2	8/5	5/7	5/7	3/8	7/9	10/6	8/11	12/7
670	2/2	9/4	6/8	5/6	3/8	7/11	11/5	10/6	4/14
700	3/2	9/4	4/5	3/9	3/10	8/12	10/7	9/11	4/13

(the interval between centers of the bands is 30 nm) in the range 400–700 nm. The mirrors are tilted to spatially separate the corresponding detectors 3, which have an individual tilt to provide optimal focusing for the entire field. For a 2.3^o field of view in the $(X, 0)$–$(–X, 0)$, $(0, Y)$–$(0, –Y)$ $(|X| = |Y|)$ directions и 3.2^o in the (X, Y)–$(–X, –Y)$, $(–X, Y)$–$(X, –Y)$ directions (Fig. 2c), the size of the image on the detectors is ~8.5 × 8.5 mm.

Results and Discussion. In the ZEMAX® program, we modeled the blur spots in non-sequential tracing mode. The halfwidth of the blur spots was estimated from the half-intensity level in the coordinate system for coordinates corresponding to imaging the coordinates of the entrance field on the detector (Fig. 2a,c). The results are given in Table 1. As we see, the halfwidth of the blur spots is not more than 15 μm, which indicates acceptable image quality. The estimate of the number of resolvable spatial elements is $>1.2 \times 10^6$. For the indicated diffraction grating parameters, the angle between the axes of beams λ = 400 nm and 700 nm is ~28.4^o, which lets us estimate the width of the passband of the polychromator as $\Delta\lambda_k \approx 18$ nm (varies according to the spectrum). By varying the slit dimensions and the dispersion of the grating, we can realize other spectral ranges, numbers of spectral bands, and $\Delta\lambda_k$ values.

Conclusions. Based on the proposed basic approach to realization of an image polychromator, we have developed a design for an instrument with passband width $\Delta\lambda \approx 18$ nm and number of resolvable spatial elements $\geq 1.2 \times 10^6$. The optical system with mirror elements provides achromaticity over a broad spectral range. The simple optical elements let us realize devices which are easy to manufacture for a broad range of applications in spatially resolved imaging spectroscopy. In particular, the indicated analytical characteristics are suitable for applications in medicine, biology, and remote sensing.

REFERENCES

1. P. Mouroulis, R. O. Green, and T. G. Chrien, *Appl. Opt.*, **39**, No. 13, 2210–2220 (2000).
2. E. S. Voropay, I. M. Gulis, A. G. Kupreyev, K. N. Kaplevsky, A. G. Kastsiukevich, A. E. Radko, and K. A. Shevcenko, *Zh. Prikl. Spektrosk.*, **77**, No. 2, 305–312 (2010) [E. S. Voropay, I. M. Gulis, A. G. Kupreyev, K. N. Kaplevsky, A. G. Kastsiukevich, A. E. Radko, and K. A. Shevcenko, *J. Appl. Spectrosc.*, **77**, 285–292 (2010)].
3. G. Lu and B. Fei, *J. Biomed. Opt.*, **19**, No. 1, 010901(1–23) (2014).
4. N. Gat, *Proc. SPIE*, **4056**, 50–64 (2000).
5. N. Hagen and M. W. Kudenov, *Opt. Eng.*, **52**, No. 9 090901(1–23) (2013).
6. K. Hashimoto, H. Mizuno, K. Nakagaw, R. Horisaki, A. Iwasaki, F. Kannari, I. Sakuma, and K. Goda, *Opt. Lett.*, **39**, No. 24, 6942–6945 (2014).
7. K. I. Tarasov, *Spectral Instruments, Second Edition* [in Russian], Mashinostroenie, Leningrad (1977), pp. 118–120.